JOURNAL OF MATERIALS SCIENCE **40** (2005) 4313–4318

Electrical behaviour of chemically activated fly ash

W. J. McCARTER*, G. STARRS, T. M. CHRISP
School of the Built Environment, Heriot-Watt University, Edinburgh, EH14 4AS, UK
E-mail: w.j.mccarter@hw.ac.uk

The temporal change in electrical properties is used to study the hydration kinetics of chemically activated fly-ash systems at room temperature. Four low-lime ashes and one high-lime ash were used in the experimental programme and the electrical response was measured in terms of the in-phase (i.e. conductance) and quadrature (i.e. capacitance) components of the sample admittance. The low-lime ash and high-lime ash exhibited markedly different electrical response. The work highlights the applicability of the testing methodology as a non-invasive, non-destructive technique in the assessment of the efficacy of a particular activator or combination of activators.

1. Introduction

The use of residual materials from certain manufacturing processes, as a partial replacement for ordinary Portland cement (OPC) in structural concrete, are beneficial on several levels,

(a) they replace that part of the cementitious binder which releases greenhouse gases and consumes the most energy in its production (viz. the OPC);
(b) they result in enhanced durability of the concrete; and,
(c) they reduce the accumulating stockpiles of these industrial by-products which is causing environmental concern.

One of the most widely available materials is pulverised fuel ash or fly-ash, which is a by-product from the generation of electricity from coal-fired power stations. The use of fly-ash, as a partial replacement for OPC in concrete is now assuming an important role in the drive for more sustainable construction materials and practices [1]. However, there is also scope for direct chemical activation of fly-ash with suitable non-OPC activators [2, 3] to produce cementitious systems of lower strengths but could be used in, for example, masonry mortars, grouts, repository backfill, non-clay bricks or slurry trench cut-off walls for containment purposes. This could further increase the utilisation of fly-ash, particularly those ashes which would not satisfy code requirements as contributing towards all (or part) of the cementitious component when used in structural concrete.

Evaluation of the setting and hardening characteristics of fly-ash with a particular activator (or combination of activators) is of considerable importance before such cementitious systems can be fully developed and exploited. Traditionally, the early hydration and reaction kinetics of OPC has been studied using isothermal conduction calorimetry. This technique has also been applied to alkali-activated blast-furnace slag systems [4–7] where heat outputs can be significant. However, as an alternative to conduction calorimetry, the prime motivation of the current work was to utilise electrical techniques as a means of continuous monitoring of the early hydration characteristics of activated fly-ash pastes and, hence, in the assessment of the efficacy of a particular activator.

The macroscopic electrical response of a cementitious system to an alternating electrical field can be represented as, $Y(f) = G(f) + j2\pi f C(f)$ where $G(\omega)$ and $C(\omega)$ represent, respectively, the conductance (real part) and capacitance (imaginary part) of the complex admittance, $Y(\omega)$, at frequency, f(Hz), and $j = \sqrt{-1}$. Whilst a considerable amount of work has been published on the electrical response of OPC [see, for example, 8–13], there is dearth of work on their application to activated fly-ash systems.

2. Experimental

2.1. Materials and sample preparation

The materials employed in the program comprised four low-lime fly-ashes (ASTM Type F) denoted FA1/2/3/4, and one high lime ash (ASTM Type C), denoted FA5. Low-lime ashes are produced from power stations using anthracite/bituminous coal, whereas high-lime ashes are produced using lignitic/sub-bituminous coal. The oxide analysis and physical properties of these materials are presented in Table I.

---

*Author to whom all correspondence should be addressed.

TABLE I Chemical and physical properties of ashes used within the experimental programme

	FA1	FA2	FA3	FA4	FA5
Fineness (% retained on 45μm sieve)	8.0	12	10	29	20
Oxide%					
SiO_2	51.0	44.3	50.5	48	33.9
Al_2O_3	27.4	24.7	24.7	27	19.4
Fe_2O_3	4.6	9.2	7.4	9	6.1
CaO	3.4	5.9	2.6	3.3	28.2
MgO	1.4	1.9	1.5	2.0	4.8
SO_3	0.7	0.69	0.8	0.6	3.0
TiO_2	1.6	1.4	1.0	0.9	1.7
K_2O	1.0	1.7	3.0	3.3	0.4
Na_2O	0.2	0.6	0.8	1.2	1.9
Loss on Ignition	5.5	1.9	5.3	4.0	0.3

Fly-ash is normally blended with OPC which then reacts with the calcium hydroxide ($Ca(OH)_2$) formed during the hydration of alite ($3CaO{\cdot}SiO_2$) and belite ($2CaO{\cdot}SiO_2$) phases in the OPC. As a result, the following standard mix formulation was used for chemical activation studies: samples were prepared by dry-blending the fly-ash and reagent grade $Ca(OH)_2$ in the ratio 4:1 (by mass) for approximately 60 seconds. Distilled water was then added to obtain a water/solids ratio of 0.5 (by mass), with the solids comprising fly-ash and $Ca(OH)_2$. Mixing then continued for a further two minutes. In the initial suite of tests, pastes were formed by mixing the solids with distilled water only; in subsequent tests, sodium sulphate (Na_2SO_4) at a dosage of 10g/100 g water (0.7 moles/l); sodium hydroxide (NaOH) at a dosage of 0.4g/100 g (0.1 moles/l) and 40/100 g water (10 moles/l), were dissolved in the mixing water.

2.2. Test cell and measurements

The pastes were compacted into plexiglas test cells of internal dimensions 50 × 50 × 50 mm. Two opposite walls of the cell had 50 × 50 × 3 mm (thick) stainless steel plate-electrodes attached. After compaction, the top surface of the sample was covered with a plexiglas sheet to prevent evaporation from the exposed surface. The cells were stored at cabinet at a temperature of 21 ± 1°C and humidity of >95%. Sample preparation and set-up procedures took 15 min.

Both conductance and capacitance measurements were taken using an impedance analyser (Hewlett Packard 4263B) operating at a frequency of 100 kHz and a drive voltage of 100 mV. Lead inductive effects were automatically nulled from the incoming data. Both the internal sample temperature and ambient laboratory temperature were monitored using a Hewlett Packard 3457A multimeter connected to temperature-matched thermistors, which gave a direct output of temperature. Data were logged automatically with all measurements (capacitance and conductance; internal sample and ambient temperatures) taken on a 10 min cycle over periods extending up to 1 week after initial mixing.

3. Discussion of results

Temporal changes in conductance (in Siemens, S) and capacitance (in Farads, F) are presented relative to the respective value taken at the start of the test. The relative change in conductance is denoted G_t/G_o where G_t represents the conductance measured at time, t after the start of the test, and G_o is the conductance at time $t = 0$; the relative change in capacitance is denoted C_t/C_o where C_t represents the capacitance measured at time, t after the start of the test, and C_o is the capacitance at time $t = 0$. G_o and C_o values are presented on the figure legends. As measurements were taken every ten minutes over the 7-day test period, for clarity, data markers have been omitted from the curves.

3.1. Fly ash/calcium hydroxide mixtures

Figs 1a and b display, respectively, the relative change in conductance and capacitance for two fly-ash/calcium hydroxide blends mixed with distilled water—FA1 and FA5, in this instance (note the change in time-scales between the Figures for FA1 and FA5).

The electrical response of the mixture will be dependent upon: (a) the fractional volume of aqueous phase; (b) the continuity and tortuosity of the interstitial aqueous path between the electrodes, and, (c) the ionic concentration within the aqueous phase. As the mixture reacts, sets and hardens, all these factors will be affected to a greater or lesser extent which, in turn, will be quantified by the electrical response of the mixture. From Fig. 1a, the conductivity of FA1 ash decreases by approximately 20% of its initial value over the 1-week test period, which would indicate an extremely sluggish reaction, hence a slow rate of strength development. The was confirmed as samples could be 'crushed' by hand at the end of the test period, any strength at this stage would be as a result of interparticle forces as opposed to the formation of products of hydration (calcium silicate hydrate) through the pozzolanic reaction.

Ash FA5, on the other hand, displays a markedly different response as there is a rapid reduction in conductance over the period $1\text{–}1\frac{1}{2}$ hours after mixing, decreasing by almost 80% of its initial value. This implies a more rapid stiffening of the mixture in comparison to FA1, and hence a more rapid increase in rigidity.

Consider also the change in capacitance for these two ashes presented in Fig. 1b. Whereas the change in capacitance for FA1 simply mimics the conductance response, the response from FA5 displays a transient peak occurring over the period when there is a rapid reduction in conductance. Interestingly, such a peak has also been observed in the setting of OPC pastes and attributed to enhanced double layer polarisation processes on the grain surface [9]. Instead, the following alternative mechanistic explanation for the transitory increase in polarizability of the FA5 system is proposed. Consider the schematic presented in Fig. 1c whereby the products of hydration (primarily calcium silicate hydrate, calcium aluminate hydrates and ettringite [14]) are depicted as outgrowths from the grain surface which result in stiffening of the mixture. Hydrates growing into the interstitial aqueous phase could be visualised

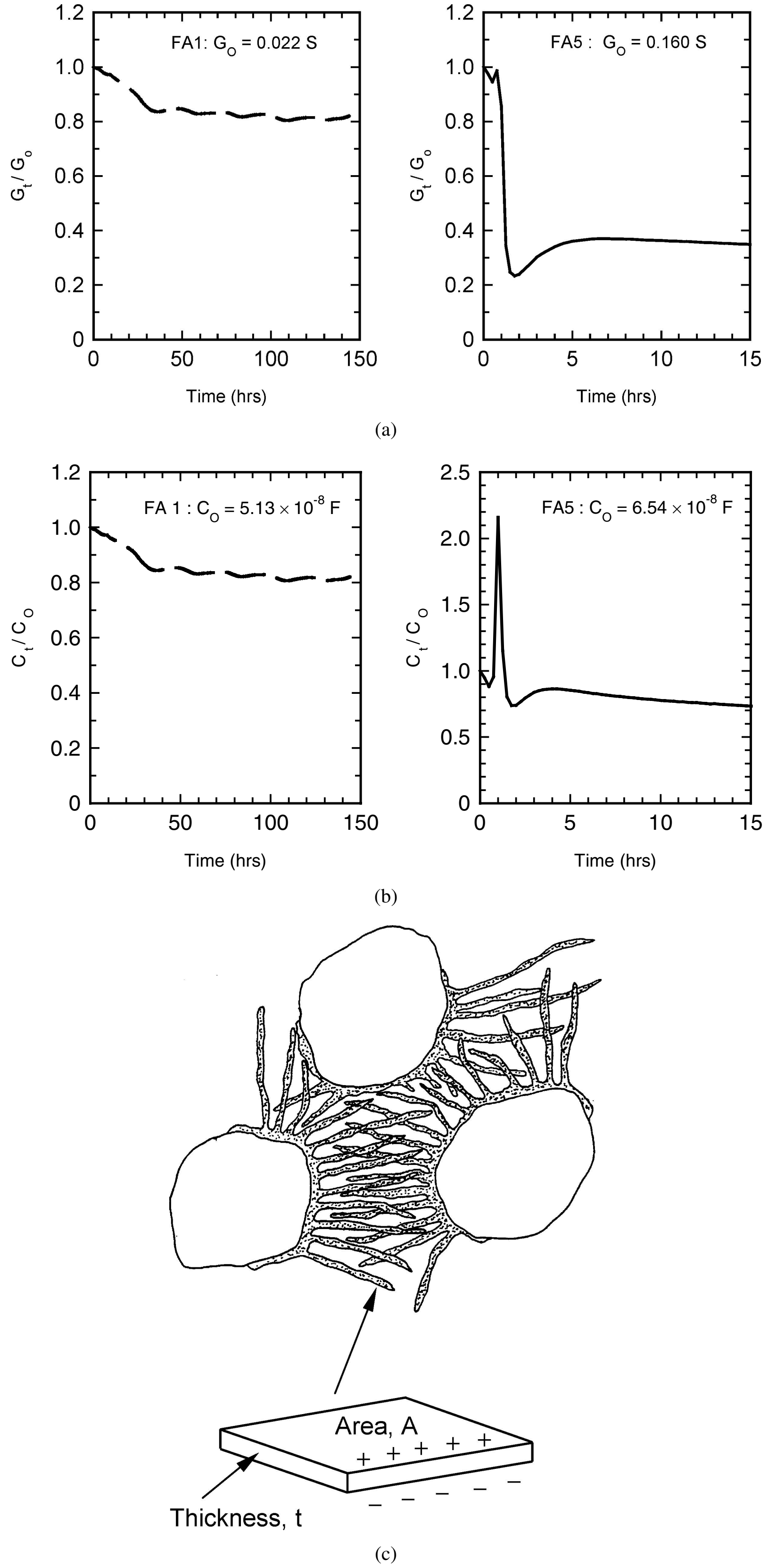

(a)

(b)

(c)

Figure 1 Relative change in (a) conductance and (b) capacitance for low-lime (FA1) and high-lime (FA5) fly-ash activated with $Ca(OH)_2$. (c) schematic diagram to explain the origin of the increase in capacitance for high-lime ash at setting.

as producing a network of thin, insulating sheets and is analogous to a network of small electrolytic capacitors, whose capacitance will be directly proportional to the exposed area, A, and inversely proportional to the thickness, t, of the hydrate (see Fig. 1c). A thin layer can produce a large capacitive effect [15] which would account for the increase in capacitance of the paste. The peak is only transitory as infilling and accretion of the pore space with hydration products result in reducing capacitance (t increases; A decreases).

Regarding the difference in response between the FA1 and FA5, this is attributable to the increased free lime content (CaO) of FA5 (see Table I), which would give the ash self-cementitious properties. It is also evident from Fig. 1 that the initial values of conductance (G_o) and capacitance (C_o) for FA5 are higher than those of FA1 and can be explained by the higher lime and alkali oxide content (Na_2O and K_2O) of FA5, which increases the ionic concentration within in the aqueous phase.

3.2. Fly ash/calcium hydroxide/sodium sulphate

The response in Fig. 1a was typical of all the low-lime ashes; however, in order to stimulate a more enhanced reactivity, in addition to blending with calcium hydroxide, Na_2SO_4 was dissolved in the gauging water. Fig. 2a presents the relative change in conductance for ashes FA1-FA4. When compared with Fig. 1a, all curves now display a central region where there is a more pronounced reduction in conductance signifying a more intense increase in rigidity of the mixture, although the time at which this decrease occurs, the time-scale over which the central region persists, and the intensity of the decrease are different for each ash.

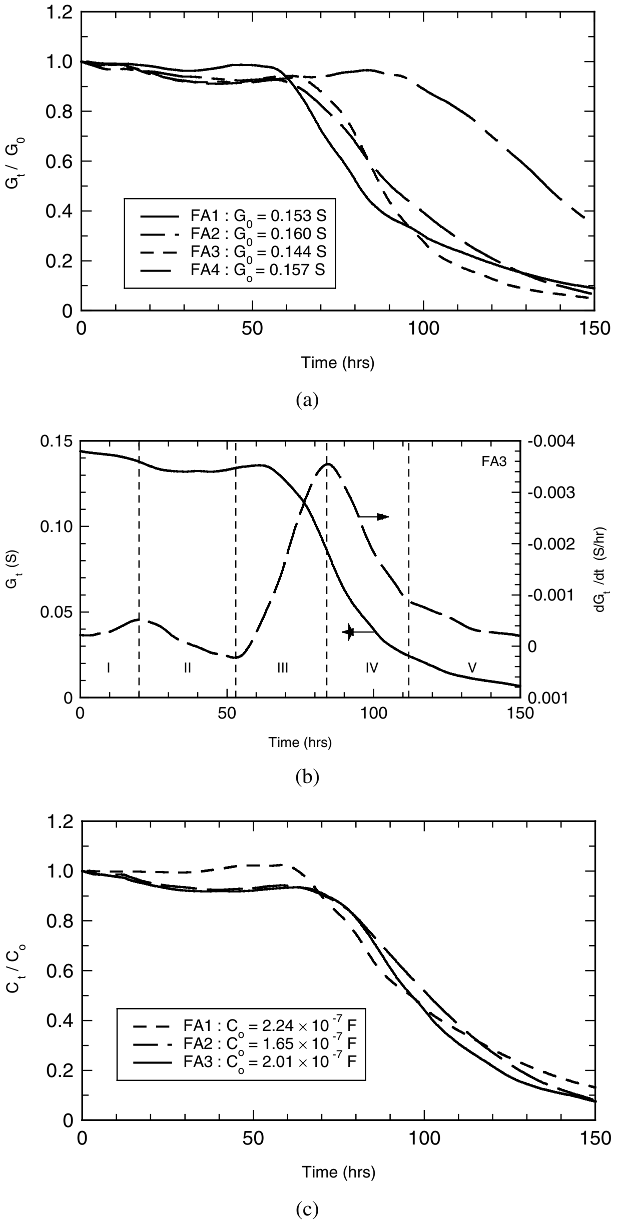

(a)

(b)

(c)

Figure 2 (a) Relative change in conductance for FA1-FA4 with addition of Na_2SO_4; (b) derivative of the conductivity (G_t) versus time curve for FA3; and (c) relative change in capacitance for FA1, FA2 and FA3.

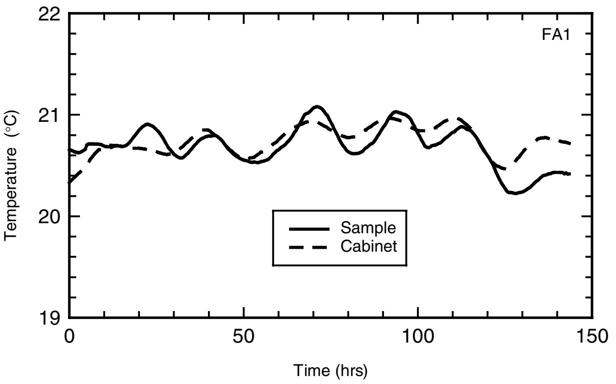

Figure 3 Temperature versus time curve for low-lime fly ash (FA1) activated with Na_2SO_4.

Examination of the derivative of the conductance versus time curves (i.e. dG_t/dt) allows delineation of several regions in the reaction process. Again, for illustrative purposes, Fig. 3b presents the resulting dG_t/dt curve for FA3. From this response, five regions can be identified over the test period: Region I, from initial gauging up to 20 h, over which time dG_t/dt increases (i.e. gets more negative) indicating initial chemical activity; Region II, from 20–53 h, where the response gradually decreases indicating reduced chemical activity; Region III, from 53 to 84 h, representing an acceleratory period with more rapid chemical activity and results in stiffening of the mixture; Region IV, from 84 to 112 h, representing a deceleration period and reduction in intensity of chemical activity; this leads into Region *V*, where there is a more gradual change in conductivity. dG_t/dt could thus be considered as indicative of the intensity of chemical activity, hence microstructural development, occurring within the mixture. In this respect, similarities can be drawn with isothermal calorimetry methods which is used to follow the hydration sequence of OPC comprising a pre-induction period; an induction or dormant period; an acceleratory period, a deceleration period followed by a diffusion controlled period.

Regarding the difference in response between low-lime/calcium hydroxide mixtures with and without Na_2SO_4, the introduction of Na_2SO_4 will increase the SO_4^{2-} concentration within the interstitial water which, in turn, would promote the formation of ettringite (AFt). The large-scale formation of AFt must be the cause of the prominent reduction in conductivity, as opposed to an enhanced pozzolanic reaction which results in the formation of calcium silicate hydrate. Regarding the latter, from Fig. 1a above, this is not the case as there is little reactivity within the fly-ash/calcium hydroxide mixture. From Fig. 2a, FA4 would appear to be the least reactive of the ashes presented as the time over which Stages I–IV occur are all increased. Considering that this is the coarsest ash (29% retained on the 45 μm sieve), the reduced surface area of the particles would account for the slower rate of reaction.

Fig. 2c displays the relative change in capacitance for ashes FA1, FA2 and FA3. As with Fig. 1a, the C_t/C_o vs. time response mimics the relative change in conductance. As the sample increases in rigidity, the irrotational binding of charges during setting reduces the polarizability of the paste; however, unlike the high-lime ash (FA5) in Fig. 1b, there is no detectable transient peak in capacitance for these ashes, even though there is a more intense crystal formation with Na_2SO_4 activation. As postulated, the occurrence of this peak is related to the rapidity of outgrowth of hydration products from the grain surface into the aqueous phase; the results would indicate that for the activator combination employed (Ca(OH)2 and Na_2SO_4), crystal growth is still too slow to cause an enhanced polarizability as observed in the high-lime ash in Fig. 1b.

3.3. Internal temperature

Fig. 3 displays the change in internal temperature for FA1 which simply follows the natural fluctuations in laboratory temperature (i.e. 21°C ± 1°C). Unlike the setting of OPC which is accompanied by a liberation of heat and consequent increase in internal temperature, little can be deduced from the temperature measurements for low-lime activated ashes. The setting process of these systems is thus too slow to cause any measurable increase in internal sample temperature and heat output techniques would be ineffective in studying the hydration of these materials.

3.4. Fly ash/calcium hydroxide/sodium hydroxide

Fig. 4 presents the relative change in conductance versus time response for FA1 using 0.1 M NaOH and 10 M NaOH dissolved in the gauging water. For comparative purposes, the response in Fig. 2a for this ash is also presented. The change in conductance over the test period suggests that 0.1 M NaOH, although producing an alkaline environment which is conducive to activation (through dissolution of the amorphous glassy phase in the ash), displays little reactivity as there is only a marginal reduction in conductivity of the mixture over the 1-week test period. The response for 10 M NaOH follows a similar pattern.

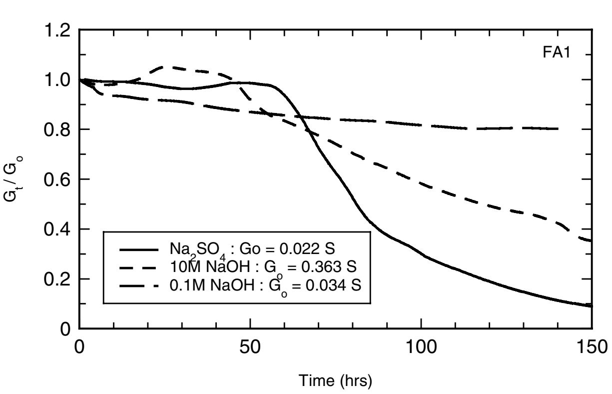

Figure 4 Relative change in conductance for NaOH activated fly ash.

The results from the electrical behaviour of these systems is corroborated by microstructural studies [16] which indicate that little reaction takes place between NaOH and fly ash (Type *F*) at room temperature; higher temperatures are required (≈90°C) for activation of such systems.

4. Concluding comments

The temporal change in conductance and capacitance of chemically activated fly-ash at room temperature were studied and new data have been presented in this respect. Of particular interest was the capacitance versus time curve for the high-lime ash and the derivative of the conductance (dG_t/dt) versus time curve for the low-lime ashes. A unique feature of the capacitance response for the high-lime ash concerned the occurrence of a transitory peak at the time of setting and a mechanistic interpretation of this feature was proposed. By utilising the dG_t/dt curve for the low-lime ashes, several stages in the early hydration process could be identified over the test period, although the duration of each stage and rate of change of electrical parameters varied between ashes.

The work demonstrates how well these electrical parameters allow monitoring of the reaction kinetics, hence increase in rigidity, of these systems. The testing methodology allows virtually continuous monitoring thereby allowing the activation effect to be quantified. The method has considerable scope for use as an additional (and complementary) tool to study, for example, the cementitious properties of by-products generally, evaluating activators and combination of activators, or the hydration of systems where there is negligible heat output.

Acknowledgements

The Authors wish to thank the Engineering and Physical Sciences Research Council (EPSRC), United Kingdom, for financial support (GR/N16365).

References

1. R. HORTON, "Factor Ten Emission Reductions: The Key to Sustainable Development and Economic Prosperity for the Cement and Concrete Industry," in Proc. 3rd CANMET/ACI Conf. on Sustainable Development of Cement and Concrete, San Francisco, 2001, SP 202-1, 1–14, (ISBN 0-87031-041-0).
2. C. SHI, *Amer. Conc. Inst., Mater. J.* **95**(5) (1998) 537.
3. J. Q. QIAN, C. SHI and Z. WANG, *Cem. Conc. Res.* **31** (2001) 1121.
4. C. SHI, *ibid.* **26**(12) (1996) 789.
5. Z. HUANHAI, W. XUEQUAN, X. ZHONGZI and T. MINGSHU, *ibid.* **23**(6) (1993) 1253.
6. C. SHI and R. L. DAY, *ibid.* **25**(6) (1995) 1333.
7. W. MA and P. W. BROWN, *ibid.* **27**(8) (1997) 1237.
8. F. TAMAS, E. FARKAS, M. VOROS and D. M. ROY, *ibid.* **17**(2) (1987) 340.
9. W. J. MCCARTER and A. AFSHAR, *J. Matls. Sci.* **23** (1986) 488.
10. P. GU, V. S. RAMACHANDRAN and J. J. BEAUDOIN, *J. Matls. Sci. Lett.* **12** (1993) 1771.

11. C. VERNET and G. NOWORYTA, “Conductometric Test for Cement-Admixture Systems.” in Proc. 9th Int. Congr. Chem. Cement, New Delhi, 1992, vol. IV, 627.
12. M. G. ABD-EL-WAHED, I. M. HELMY, H. EL-DIDAMONY and D. EBIED, *J. Matls. Sci. Lett.* **12** (1993) 40.
13. P. PU, V. S. RAMACHANDRAN and J. J. BEAUDOIN, *ibid.* **14** (1995) 503.
14. J. BENSTED and P. BARNES, “Structure and Performance of Cements,” 2nd ed. (Spon Press, London, 2002) (ISBN 0–419-23330-X).
15. B. J. CHRISTENSEN, R. T. COVERDALE, R. A. OLSEN, S. J. FORDE, E. J. GARBOCZI, H. M. JENNINGS and T. O. MASON, *J. Amer. Ceram. Soc.* **77**(11) (1994) 2789.
16. A. KATZ, *Cem. and Conc. Res.* **28**(2) (1998) 197.

Received 30 September 2003
and accepted 7 March 2005